Institute of metal physics
Skolkovo Institute of Science and Technology

Electrides: in pursuit of correlations

Dmitry Novoselov

November 12

19th ONLINE USPEX workshop
Moscow, Russia

Supported by the Russian Scientific Foundation grant No. 19072-30043 “Computational materials design laboratory”

What color is an electron?

- Blue
- Green
- Yellow

VOL. XXX. SEPTEMBER, 1908. No. 9

THE JOURNAL

OF THE

American Chemical Society

[CONTRIBUTIONS FROM THE RESEARCH LABORATORY OF PHYSICAL CHEMISTRY OF THE MASSACHUSETTS INSTITUTE OF TECHNOLOGY, No. 36]

SOLUTIONS OF METALS IN NON-METALLIC SOLVENTS; IV.[1] MATERIAL EFFECTS ACCOMPANYING THE PASSAGE OF AN ELECTRICAL CURRENT THROUGH SOLUTIONS OF METALS IN LIQUID AMMONIA. MIGRATION EXPERIMENTS.

BY CHARLES A. KRAUS.

Received July 15, 1908.

The negative ion constitutes a new species of anion. It consists of a negative charge, an electron, surrounded by an envelope of solvent molecules. The electron is thus in equilibrium with ammonia according to the equation:

$$\varepsilon^- . (NH_3)_x \rightleftharpoons \varepsilon^- + xNH_3.$$

At the same time the electron is in equilibrium with the metal cations and the neutral metal atoms according to the equation

$$M^+ + \varepsilon^- \rightleftharpoons M_a.$$

where M^+ signifies the cation and M_a the neutral atom.

BOSTON, July 14, 1908.

Independent electrons

The absorption band of a solvated electron:
in water and ammonia 720 nm
in methanol 625 nm
in ethanol 680 nm
in decanol 650 nm

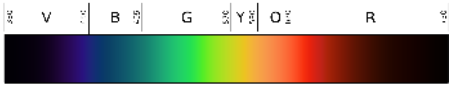

Sodium dissolves in liquid ammonia (NH_4^+)

$Na + 6\ NH_3 \rightarrow [Na(NH_3)_6]^+ \cdot e^-$

Cotton, F. A.; Wilkinson, G. (1972). Advanced Inorganic Chemistry. John Wiley and Sons Inc. ISBN 978-0-471-17560-5.

Lithium solution in liquid ammonia:

- the dark blue color corresponds to the insulating state
- golden (concentration more than 3 moles) - conductor

Schindewolf, U. (1968). "Formation and Properties of Solvated Electrons". 7 (3): 190–203. doi:10.1002/anie.196801901.
Cotton, F. A.; Wilkinson, G. (1972). Advanced Inorganic Chemistry. John Wiley and Sons Inc. ISBN 978-0-471-17560-5.

Halite (NaCl)

(derived from the Ancient Greek word for salt, ἅλς (háls))

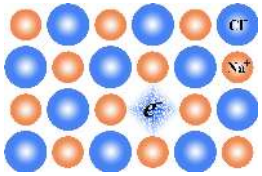

First crystalline electride $Cs^+(18\text{-Crown-}6)_2\cdot e^-$

J. Am. Chem. Soc. **1983**, *105*, 6490–6491

Cesium 18-Crown-6 Compounds. A Crystalline Ceside and a Crystalline Electride

Ahmed Ellaboudy and James L. Dye*

Department of Chemistry, Michigan State University East Lansing, Michigan 48824

Patrick B. Smith

Dow Chemical Company Midland, Michigan 48640

Received July 22, 1983

J. Am. Chem. Soc. **1986**, *108*, 3534–3535

First Electride Crystal Structure

Steven B. Dawes, Donald L. Ward, Rui He Huang, and James L. Dye*

Department of Chemistry, Michigan State University East Lansing, Michigan 48824

Received January 21, 1986

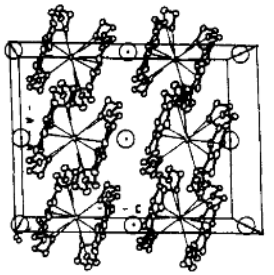

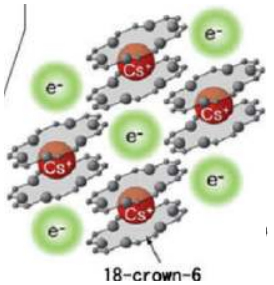

Figure 1. ORTEP stereo packing diagram of $Cs^+(18C6)_2\cdot e^-$. The anionic hole centers are indicated by the symbol ⊙.

First inorganic electride $[Ca_{24}Al_{28}O_{64}]^{4+}4e^-$

$I\bar{4}3d$

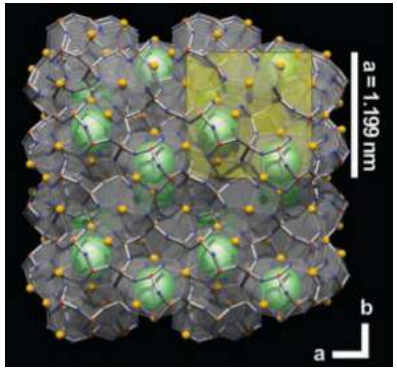

Matsuishi S, Toda Y, Miyakawa M, Hayashi K, Kamiya T, Hirano M, Tanaka I, Hosono H. Science 301, 626–629 (2003)

$$n_e \sim 2.33 \cdot 10^{21} cm^{-3}$$

Excess electron

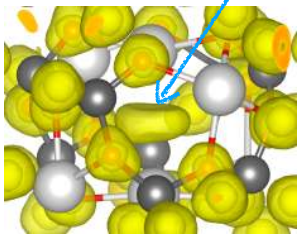

ELF

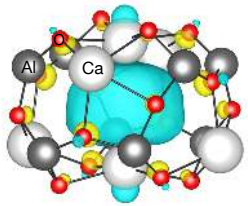

Spatial distribution of the MLWF describing the electride state.

Applications

- **Electron emitters**
  Huang, R. H. & Dye, J. L. Low temperature (-80°C) thermionic electron emission from alkalides and electrides. Chem. Phys. Lett. 166, 133–136 (1990).
- **Superconductors (room temperature!)**
  Hosono, H. et al. Superconductivity in room-temperature stable electride and high-pressure phases of alkali metals. Philos. Trans. R. Soc. A Math. Phys. Eng. Sci. 373, (2015).
- **Battery anodes**
  Hu, J. et al. 2D Electrides as Promising Anode Materials for Na-Ion Batteries from First-Principles Study. ACS Appl. Mater. Interfaces 7, 24016–24022 (2015).
- **Optics (Ca_2N as a natural hyperbolic metamaterial)**
  Guan, S., Huang, S. Y., Yao, Y. & Yang, S. A. Tunable hyperbolic dispersion and negative refraction in natural electride materials. Phys. Rev. B 95, 1–6 (2017).
- **Cathode material in fluorescent lamps (mayenite)**
  Watanabe, S. et al. Secondary electron emission and glow discharge properties of 12CaO7Al2O3 electride for fluorescent lamp applications. Sci. Technol. Adv. Mater. 12, (2011).
- **Radioactive waste storage (mayenite encapsulates volatile fission products)**
  Kuganathan, N., Chroneos, A. & Grimes, R. W. The encapsulation selectivity for anionic fission products imparted by an electride. Sci. Rep. 9, 1–11 (2019).
- **Catalysts for a range of applications**
  - **mayenite activate and split carbon dioxide at room temperature**
    Toda, Y. et al. Activation and splitting of carbon dioxide on the surface of an inorganic electride material. Nat. Commun. 4, 1–8 (2013).
  - **ammonia production**
    Kitano, M. et al. Ammonia synthesis using a stable electride as an electron donor and reversible hydrogen store. Nat. Chem. 4, 934–940 (2012).

1908

Solvated electrons

$e\ e\ e$

1983-86

Organic electrides

J. Am. Chem. Soc. 1996, 118, 7329-7336

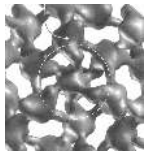

$[Cs^+(15\text{-crown-5})(18\text{-crown-6})e^-]_6$

2003

Inorganic electrides

Science 301, 626–629 (2003)

Mayenite

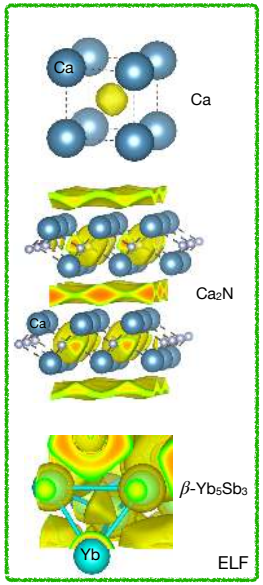

...

Challenge

- ☑ Magnetic fluctuations (Ca_2N, Yb_5Sb_3)
- ☑ Broadening and renormalisation of the electride bands (Ca_2N)
- ☑ Lifetime of excited electride states (Yb_5Sb_3)
- ☑ Thermodynamically stable magnetic phase (Gd_2C)
- ☑ Van der Waals interaction between layers that arises from the dipole-induced dipole interaction which is entirely due to correlation between electride electrons (2D-electrides)
- ☑ Structure transitions inaccessible in single-particle approximations (Ca, Ca_2N)
- ☑ Insulator-metal transitions (Yb_5Sb_3)

What is the role of Coulomb correlations between anionic electrons in the formation of electride properties?

Approach and tools

		Quantum-ESPRESSO	*Giannozzi, P. et al. QUANTUM ESPRESSO: a modular and open-source software project for quantum simulations of materials. J. Phys. Condens. Matter 21, 395502 (2009).*
$\varepsilon(\mathbf{k})$	**DFT**		
		VASP	*Kresse, G. & Furthmüller, J. Efficient iterative schemes for ab initio total-energy calculations using a plane-wave basis set. Phys. Rev. B 54, 11169–11186 (1996).*
H_{GGA}	**MLWF**	**Wannier90**	*Mostofi, A. A. et al. An updated version of wannier90: A tool for obtaining maximally-localised Wannier functions. Comput. Phys. Commun. 185, 2309–2310 (2014).*
		AMULET	*www.amulet-code.org*
Σ, G	**DMFT**	**CT-QMC Hybridization expansion**	*Werner, P. & Millis, A. J. Hybridization expansion impurity solver: General formulation and application to Kondo lattice and two-orbital models. Phys. Rev. B 74, 155107 (2006).*

Structure transitions in elemental calcium

Li, B. et al. Calcium with the β-tin structure at high pressure and low temperature. Proc. Natl. Acad. Sci. U.S.A. 109, 16459–16462 (2012).

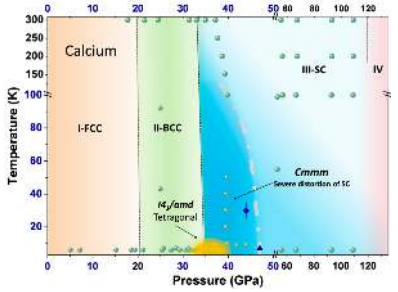

Phase diagram of Ca at high pressure and low temperature.

Oganov, A. R. et al. Exotic behavior and crystal structures of calcium under pressure. Proc. Natl. Acad. Sci. 107, 7646–7651 (2010).

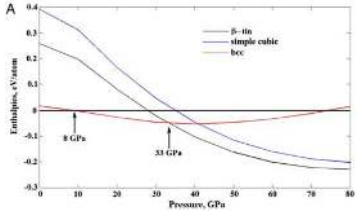

Enthalpies of the bcc, sc, and I41/amd (β-tin phase) structures (relative to fcc).

DFT method is not able to reproduce the transition to a simple cubic phase

What is the nature of the stability of the SC structure at low temperatures?

Electride formation in Ca

Oganov, A. R. et al. Exotic behavior and crystal structures of calcium under pressure. Proc. Natl. Acad. Sci. 107, 7646–7651 (2010).

Valence ELF (including semicore 3s and 3p-states) of fcc-Ca at 1 atm and 18 GPa.

«ELF has maxima not only at the nuclei, but also in the octahedral voids between them. These maxima become much more pronounced on increasing pressure»

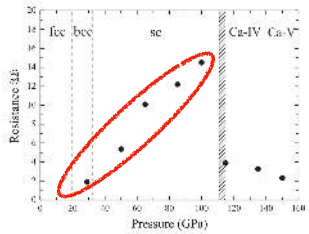

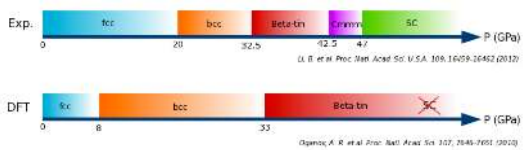

Yabuuchi, T. et al., J. Phys. Soc. Japan 74, 2391 (2005).

Could the electride states and correlations be responsible for SC structure stability?

Charge density of Ca under pressure

0D-electride
SC

1D-electride
β-tin

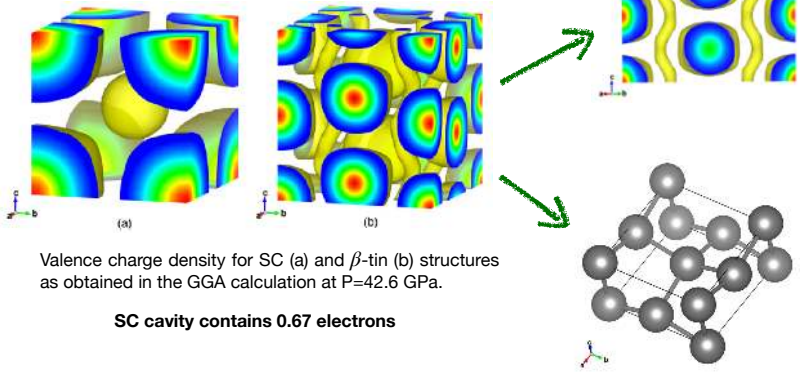

Valence charge density for SC (a) and β-tin (b) structures as obtained in the GGA calculation at P=42.6 GPa.

SC cavity contains 0.67 electrons

SC phase of calcium is a zero-dimensional electride

$I4_1/amd$

Interstitial states in the bands of Ca

Wannier function of *s*-symmetry centered on the cubic void within the SC cell (left) and WFs of d_{xz}, d_{xy}-symmetry (right). Ca atoms denoted with red spheres.

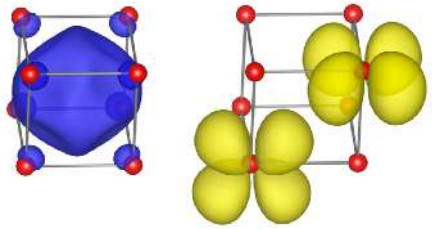

Band structure of SC Ca and contribution of the WF with s-symmetry centered on interstice to the Bloch states.

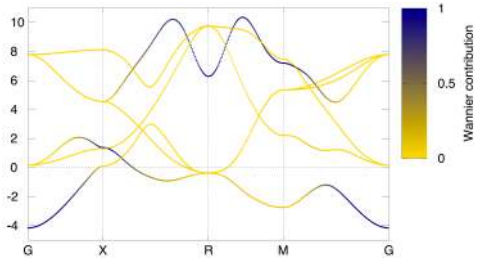

Coulomb parameter U and DMFT correlation energy in Ca

The constrained DFT procedure: U=0.47eV

Anisimov, V. I. & Gunnarsson, O. Density-functional calculation of effective Coulomb interactions in metals. Phys. Rev. B 43, 7570–7574 (1991).

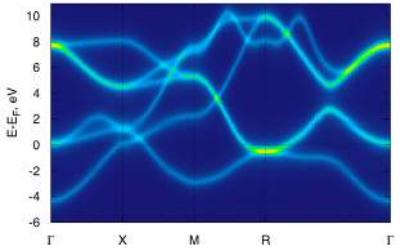

ARPES for the SC structure obtained in the DFT+DMFT calculation for V= 18.23 Å^3.

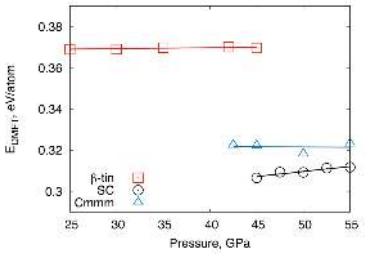

DMFT energy correction.

The total energy correction due to the correlation effects almost does not depend on applied pressure for the considered structures.

Correlations and phase transitions in Ca

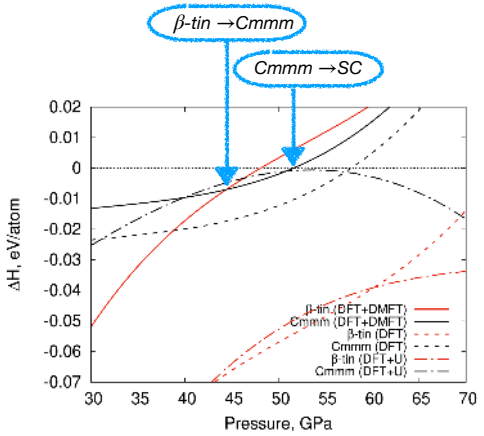

Enthalpy of beta-tin (red) and Cmmm (black) phases of Ca under pressure obtained in the DFT (dashed lines) and DFT+DMFT (solid lines) with respect to SC shown by zero line.

Correlation effects are strong enough to result in the correct phase sequence in Ca under pressure.

Novoselov, D. Y., Korotin, D. M., Shorikov, A. O., Oganov, A. R. & Anisimov, V. I. Weak Coulomb correlations stabilize the electride high-pressure phase of elemental calcium. J. Phys. Condens. Matter 32, 445501 (2020).

First 2D electride $[Ca_2N]^+ \cdot e^-$

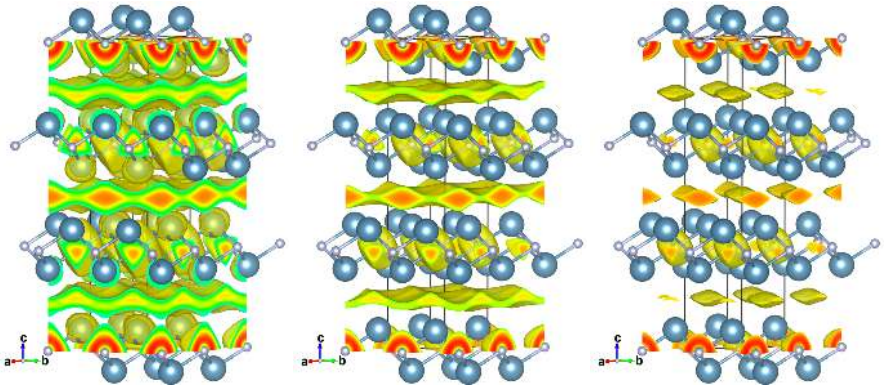

ELF=0.25 ELF=0.5 ELF=0.65

Excess electrons are in a quasi-two-dimensional region between Ca^{2+} ions located in the outermost positions of each layer, which provides electrostatic stability for electrons.

First 2D electride $[Ca_2N]^+ \cdot e^-$

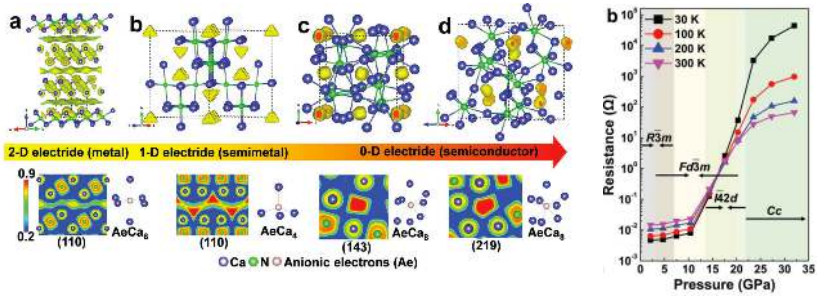

Tang, H. et al. Metal-to-Semiconductor Transition and Electronic Dimensionality Reduction of Ca_2N Electride under Pressure. Adv. Sci. 5, 2–7 (2018).

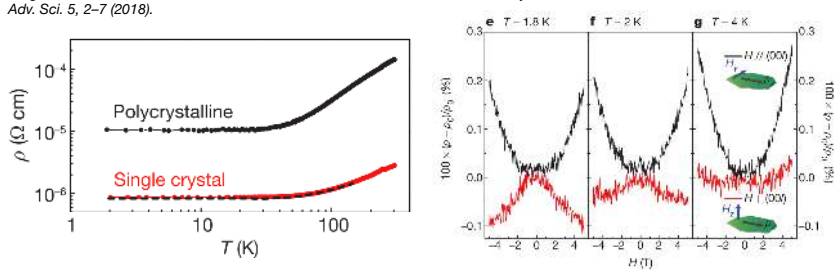

K. Lee, S. W. Kim, Y. Toda, S. Matsuishi and H. Hosono, Nature, 2013, 494, 336–340.

Experimental evidence for anionic excess electrons in Ca_2N and the theoretical challenges

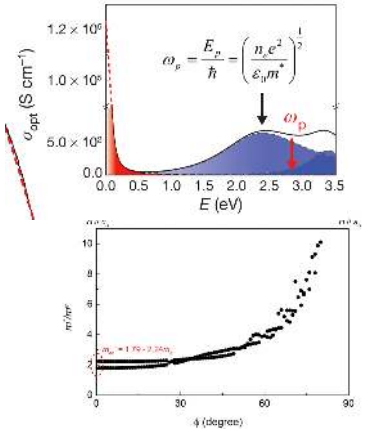

$m^*/m \approx 1.8 - 2.5$

ARPES

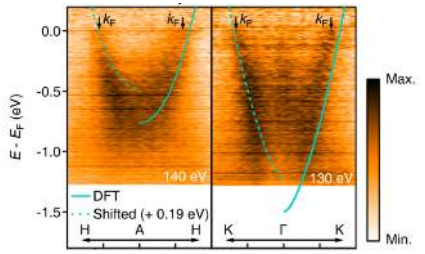

Oh, J. S. et al. J. Am. Chem. Soc. 138, 2496–2499 (2016).

How the Coulomb correlations affect the physical properties of Ca_2N?
How strong are the correlations?

K. Lee, S. W. Kim, Y. Toda, S. Matsuishi and H. Hosono, Nature, 2013, 494, 336–340.

Interlayer states in Ca_2N

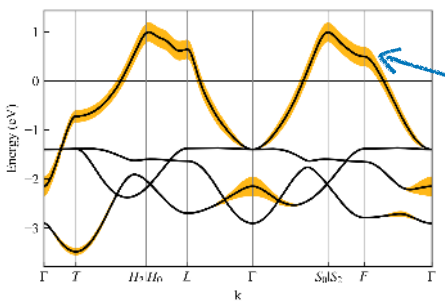

Band structure of Ca_2N (black lines). The contribution to the Bloch states by the maximally localized Wannier function with s-symmetry centered on the electride layers is shown in yellow.

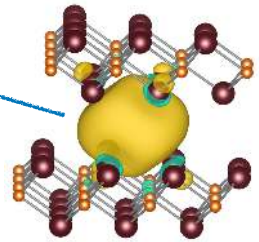

Spatial distribution of the MLWF describing the electride state. The Ca and N atoms are shown in reddish-purple and orange, respectively.

The electrical conductivity of Ca_2N is due to the electrons enclosed in the space between the layers.

Self-energy and Green's functions of electride states in Ca_2N

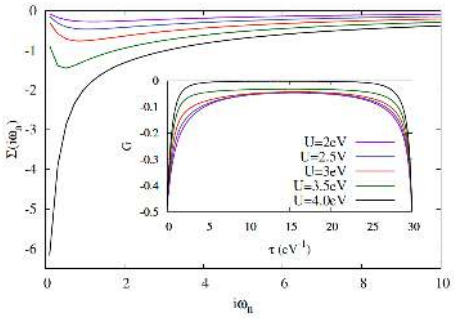

Imaginary part of self-energy as a function of Matsubara frequencies at β=30 eV^{-1} for different values of Coulomb parameter U and corresponding Green's functions in the inset.

The value of Green function at half of beta indicates the metallic character of conductivity at intermediate values of U.

Spectral functions of Ca_2N

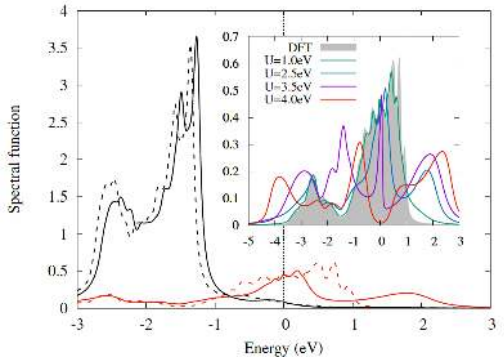

Spectral functions obtained using DFT (dashed lines) and DFT+DMFT (solid lines) for β=30 eV^{-1} and U=2.5 eV resolved for the electride (red) and p-N (black) states. The spectral functions of the electride states obtained using DFT and DMFT for different values of U are shown in the inset. Zero corresponds to the Fermi energy.

An increase of U up to 2.5 eV leads to a renormalization of the spectral weight and narrowing of the band around the Fermi level.

Electron mass enhancement and U in Ca_2N

$$m^*/m = 1 - \frac{\partial \Sigma}{\partial \omega}|_{\omega=0}$$

TABLE I. Effective electron mass enhancement m^*/m and the Fermi level shift relative to DFT value obtained using DMFT at $\beta = 30$ eV^{-1}. The experimentally determined electron mass enhancement is 1.9-2.5 [7].

	U=2 eV	U=2.5 eV	U=3 eV	U=3.5 eV
m^*/m	1.74	2.35	3.62	9.21
ΔE_F	0.07	0.09	0.12	0.16

Linear response: U=2.78 eV

At U=2.5 eV, the m^*/m equals 2.35m_e, which agrees better with the experimental value of 1.9–2.5m_e and the paramagnetic solution with a local instant squared magnetic moment of 0.76μ_B per electride site.

Exp: K. Lee, S. W. Kim, Y. Toda, S. Matsuishi and H. Hosono, Nature, 2013, 494, 336–340.

ARPES of Ca_2N

ARPES obtained in DMFT calculations at β=60 eV^{-1} with U=2.5 eV. Band structure from DFT calculations is shown by solid red lines.

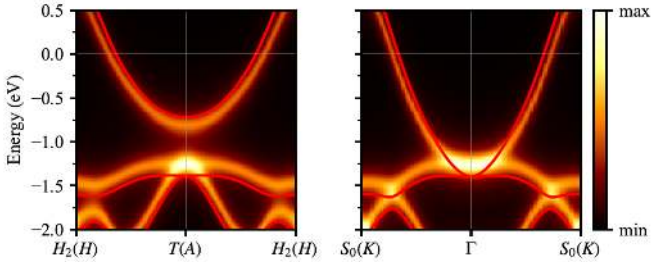

Dynamic Coulomb correlations between the confined electrons lead to the shift of the Fermi level and renormalization of the bands, as well as to their smearing.

Magnetic properties of Ca_2N

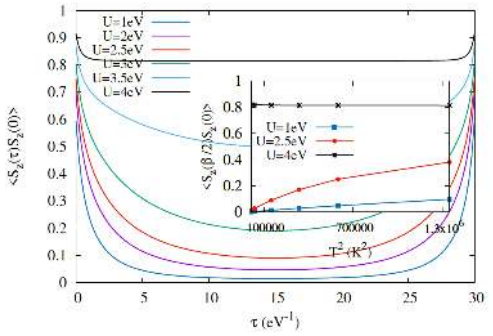

Local spin-spin correlation functions in the imaginary-time domain obtained using DFT+DMFT at β=30 eV^{-1} for different values of the Coulomb parameter U. Inset: Dependence of the spin-spin correlation function on T^2 at $\tau=\beta/2$ and U=1, 2.5, and 4 eV.

$$U = 4eV : \langle \mathbf{S}_z(\tau)\mathbf{S}_z(0)\rangle \approx S^2$$

For U=2.5 eV, the curve of $\langle S_z(\beta/2)S_z(0)\rangle$ lies between those for U=1 and 4 eV, which indicates an intermediate regime with partially localized electrons that is closer to the Fermi liquid at high temperatures.

Local spin susceptibility of Ca_2N

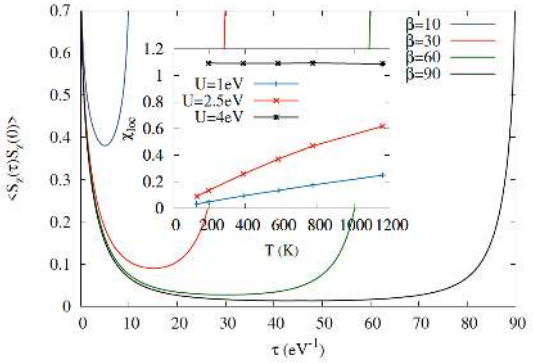

$$\chi_{\text{loc}} = g_s^2/3 \cdot \int_0^\beta d\tau \langle \mathbf{S}(0)\mathbf{S}(\tau)\rangle$$

$$g_s = 2$$

Local spin-spin correlation functions in the imaginary-time domain obtained using DFT+DMFT at U=2.5 eV for different values of β. Inset: Temperature dependence of the local spin susceptibility at U=1, 2.5, and 4 eV.

Partially localized and relatively large magnetic moments are present in the interstitial sites for U=2.5 eV.

Magnetic susceptibility of Ca_2N

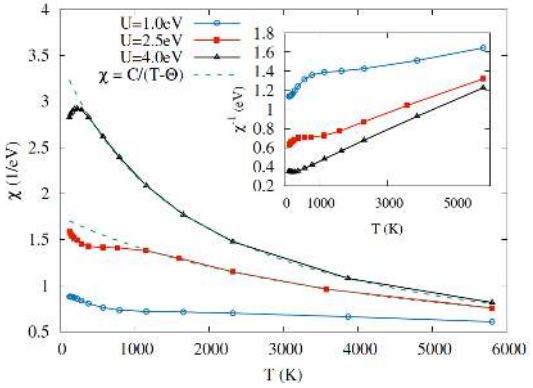

$$\chi(T) = m(T)/H_z$$

$$m(T) = \sum_m (n_m^\uparrow - n_m^\downarrow)$$

Temperature dependencies of the uniform magnetic susceptibility and its inverse (in the inset).

The Stoner-type ferromagnetic instability prevails at low temperatures, and an increase in the temperature leads to a growth in the localization of the moments and a strengthening of the antiferromagnetic interaction.

Dimorphic $[Yb_5Sb_3]^{+}\cdot e^{-}$

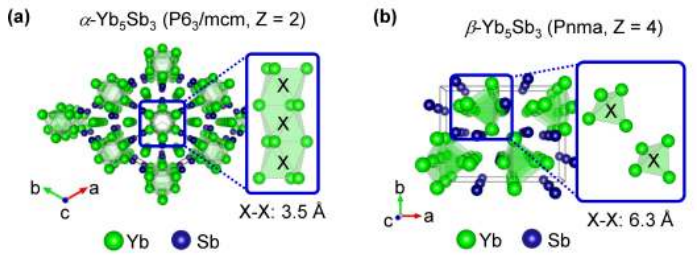

Yangfan Lu, Junjie Wang, Jiang Li, Jiazhen Wu, Shu Kanno, Tomofumi Tada and Hideo Hosono PRB 98, 125128 (2018).

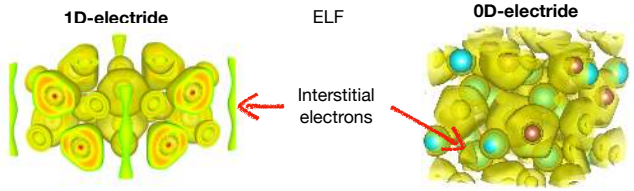

The smaller dimension of the cavities leads to a more pronounced localization of the electride states.

Exp. and DFT+U

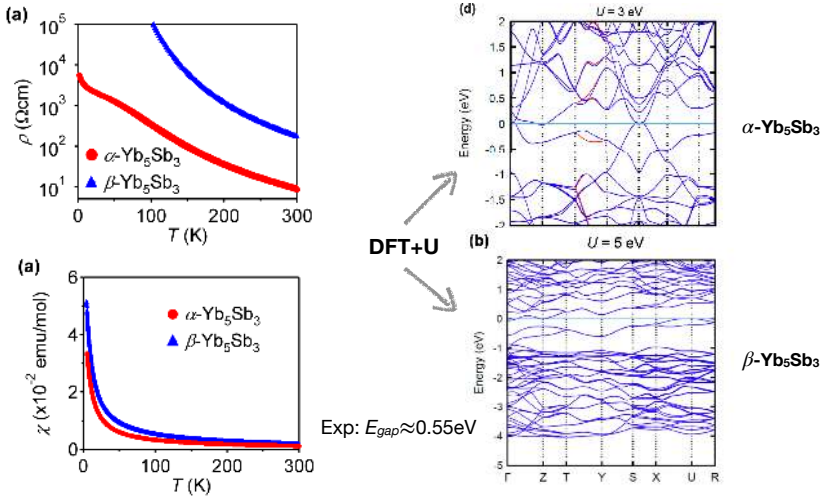

Exp: E_{gap}≈0.55eV

Yangfan Lu, Junjie Wang, Jiang Li, Jiazhen Wu, Shu Kanno, Tomofumi Tada and Hideo Hosono PRB 98, 125128 (2018).

What is the role of electride states in semiconductor behavior and magnetism in β-Yb_5Sb_3?

Interstitial electronic states of β-Yb_5Sb_3

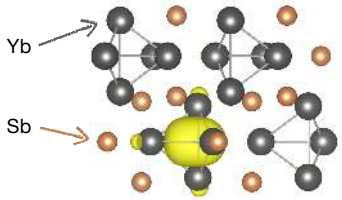

Crystal structure of β-Yb_5Sb_3 with isosurface of one MLWF localized in the tetrahedral cavity.

Spatial distribution of the MLWF describing the electride state. The Yb and Sb atoms are shown in dark-grey and orange, respectively.

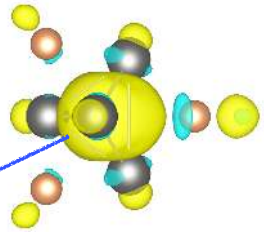

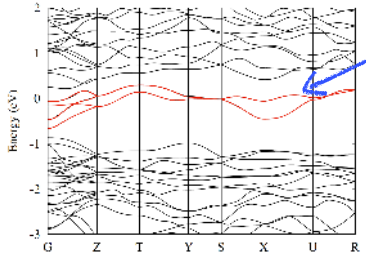

DFT band structure of β-Yb_5Sb_3 (black lines). Fermi level corresponds to zero.

The contribution to the Bloch states by the maximally localized Wannier function centered on the tetrahedral interstitial voids is shown in red.

Metal-insulator Mott transition in β-Yb_5Sb_3

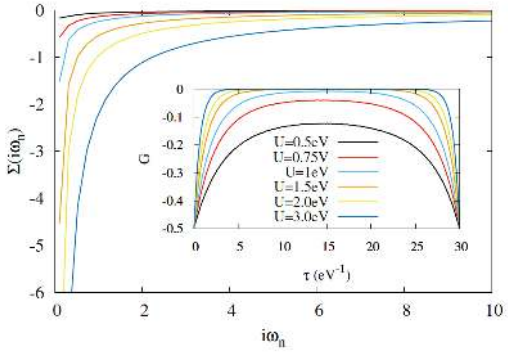

Imaginary part of self-energy as a function of Matsubara frequencies at β =30 eV^{-1} for different values of Coulomb parameter U and corresponding Green's functions in the inset for one impurity.

$G(\beta/2)$ indicates the evolution from metallic to the insulating character of conductivity with the growth of U.

Metal-insulator Mott transition in β-Yb_5Sb_3

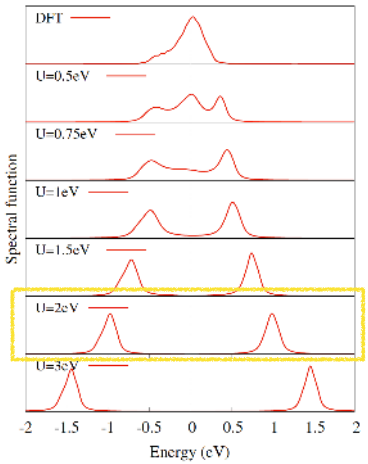

The Mott insulator state in β-Yb_5Sb_3 electride exists due to the Coulomb interactions of the electrons not related to specific sites of the crystal lattice

Exp: E_{gap}≈0.55eV

Yangfan Lu, Junjie Wang, Jiang Li, Jiazhen Wu, Shu Kanno, Tomofumi Tada and Hideo Hosono PRB 98, 125128 (2018).

Spectral functions obtained using DFT (top panel) and DFT+DMFT for different values of U at β=30 eV^{-1}. Zero corresponds to the Fermi energy.

Semiconducting behavior of β-Yb_5Sb_3

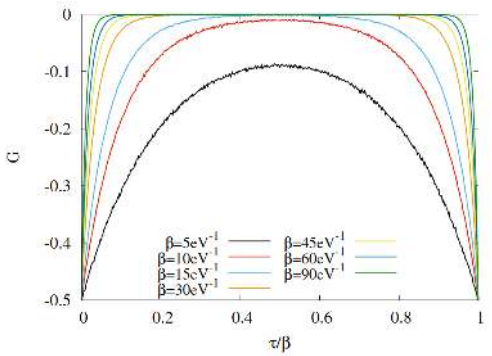

Temperature decreases $T = \frac{1}{k_B \beta}$

Green's functions at U=2 eV and different values of the β parameter

The semiconducting behavior of β-Yb_5Sb_3 is caused by Coulomb correlations between the electride electrons

Localization and magnetism in β-Yb_5Sb_3

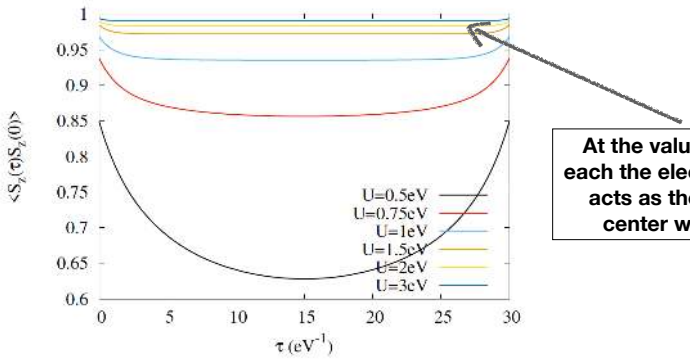

At the value of U=2 eV each the electride density acts as the magnetic center with S=1/2.

Local spin-spin correlation functions $\langle \mathbf{S}_z(\tau)\mathbf{S}_z(0)\rangle$ in the imaginary-time domain obtained using DFT+DMFT at β=30 eV^{-1} for different values of the Coulomb parameter U

Localization and magnetism in β-Yb_5Sb_3

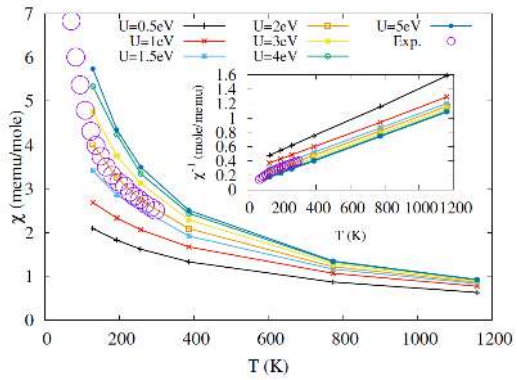

$\chi(T) = m(T)/H_z$

$m(T) = \sum_m (n_m^{\uparrow} - n_m^{\downarrow})$

The model mainly derived from the interstitial anionic electronic states properly describes the magnetic features of β-Yb_5Sb_3 with the moderate value of the Coulomb parameter U.

Temperature dependencies of the uniform magnetic susceptibility $\chi(T)$ and its inverse (in the inset) for different values of U as well as the experimental data [1] shown by the violet circles.

[1] Yangfan Lu, Junjie Wang, Jiang Li, Jiazhen Wu, Shu Kanno, Tomofumi Tada and Hideo Hosono PRB 98, 125128 (2018).

Conclusion remarks

- Electride states can be correlated while the strength of correlations can vary from weak to strong.
- Coulomb correlations between electrons described by electride states can directly be related to the most interesting physical properties of such materials including structural transitions, metal-insulator transitions, strong interstitial local magnetic moments and magnetic fluctuations.
- Properly describing the electride states and taking into account dynamical correlation effects make it possible to correctly model both already known electrides and to search for and predict new ones.

Thank you for your attention!